DOI: 10.3969/j. issn. 1673-5188. 2016. 04. 001
http://www.cnki.net/kcms/detail/34.1294.TN.20161014.0955.002.html, published online October 14, 2016

Evaluation of Preamble Based Channel Estimation for MIMO-FBMC Systems

Sohail Taheri[1], Mir Ghoraishi[1], XIAO Pei[1], CAO Aijun[2], and GAO Yonghong[2]
(1. 5G Innovation Centre, Institute for Communication Systems (ICS), University of Surrey, Guildford, Surrey GU2 7XH, United Kingdom;
2. ZTE Wistron Telecom AB, Kista, Stockholm 164 51, Sweden)

Abstract

Filter-bank multicarrier (FBMC) with offset quadrature amplitude modulation (OQAM) is a candidate waveform for future wireless communications due to its advantages over orthogonal frequency division multiplexing (OFDM) systems. However, because of orthogonality in real field and the presence of imaginary intrinsic interference, channel estimation in FBMC is not as straightforward as OFDM systems especially in multiple antenna scenarios. In this paper, we propose a channel estimation method which employs intrinsic interference cancellation at the transmitter side. The simulation results show that this method has less pilot overhead, less peak to average power ratio (PAPR), better bit error rate (BER), and better mean square error (MSE) performance compared to the well-known intrinsic approximation methods (IAM).

Keywords

channel estimation; filter-bank multicarrier (FBMC); multiple-input multiple-output (MIMO); offset quadrature amplitude modulation (OQAM); wireless communication

1 Introduction

Orthogonal frequency division multiplexing (OFDM) has been widely used in communication systems in the last decade. This is because of its immunity to multipath fading and simplicity of channel estimation and data recovery with a low complexity single-tap equalization, and also suitability for multiple-input multiple-output (MIMO) systems [1]. However, it suffers from disadvantages such as sensitivity to carrier frequency offset (CFO), significant out-of-band radiation, and cyclic prefix overhead. In the presence of CFO, there is loss of orthogonality between subcarriers leading to inter carrier interference (ICI). Moreover, to efficiently use the available spectrum, a waveform with very low spectral leakage is needed.

Because of the OFDM shortcomings, filter-bank multicarrier (FBMC) modulation combined with offset quadrature amplitude modulation (OQAM) has drawn attention in the last decade [2], [3]. Regardless of the higher complexity compared to OFDM, FBMC (known as OFDM/OQAM and FBMC/OQAM in the literature) provides significantly reduced out-of-band emissions, robustness against CFO [4], and under certain conditions, better spectral efficiency as there is no need to use cyclic prefix (CP) [5]. These advantages come from well localized prototype filters in time and frequency domain for pulse shaping. Accordingly, FBMC can be a promising alternative to conventional radio access techniques to improve wireless access capacity.

On the other hand, as orthogonality in FBMC systems only holds in the real field, received symbols are contaminated with an imaginary intrinsic interference term coming from the neighbouring real symbols. The interference becomes a source of problem in channel estimation and equalization processes, especially in MIMO systems. The pilot symbols used for channel estimation should be protected from interference as the receiver has no knowledge about their neighbours to estimate the amount of interference. These protections cause overheads when designing a transmission frame. In a preamble-based approach, the preamble should be protected from the subsequent data transmission and the previous frame by inserting null symbols, which causes longer preamble and thus more overhead compared to OFDM. This is also true for scattered pilots where the neighbouring data symbols contribute to the interference on the pilots [6]. In this scenario, typically one or two time-frequency points adjacent to the pilots are used to cancel the interference on the pilots [7]–[10].

Interference Approximation Method (IAM) for preamble-

This work is supported by ZTE Industry-Academia-Research Cooperation Funds under Grant No. Surrey-Ref-9953.

based channel estimation in single-input, single-output (SISO) systems was first introduced in [11]. The preamble was named IAM-R in the literature, where R denotes real-valued pilots. Alternatively, IAM-I and IAM-C were introduced in [12], [13], where I and C stand for imaginary and complex pilots. Those preamble based channel estimation schemes were extended to FBMC-MIMO systems in [14]. In IAM-I and IAM-C, pilots on each subcarrier interfere with their adjacent subcarriers in a constructive way. That is, these methods use the intrinsic interference to enhance amplitude of the pilots. As a result, better performance of channel estimation is achieved. Despite good performance, IAM methods suffer from increased pilot overhead, i.e., a number of zero symbols are required to protect the pilot symbols from the interference of their adjacent symbols. While the number of pilot symbols is equal to the number of antennas, the total number of symbols in the preamble will be more than twice the number of transmit antennas.

This paper proposes a channel estimation method with reduced preamble overhead compared to the IAM family. The idea was first introduced in [15] for MIMO-OFDM. Applying this method to MIMO-FBMC with spatial multiplexing needs further consideration to cancel intrinsic interference. By using basic idea of zero forcing from single antenna, this method has modest computation complexity, while it can outperform IAM methods in terms of peak to average power ratio (PAPR), bit error rate (BER), and mean square error (MSE) under perfect synchronization conditions and in presence of carrier frequency offset.

The rest of this paper is organized as follows: Section 2 reviews the MIMO-FBMC systems, the effect of intrinsic interference, and the conventional channel estimation methods. In Section 3, the new method for channel estimation is proposed and Section 4 shows the results and comparisons with IAM methods. Finally, conclusions are drawn in Section 5.

2 MIMO-FBMC System

2.1 System Model

FBMC systems are implemented by a prototype filter $g(t)$ and synthesis and analysis filter-banks in transmitter and receiver side respectively. The real and imaginary parts of complex symbols are separated in two different branches where they are modulated in FBMC modulators as real symbols. Therefore, at a specific time, each subcarrier in this system carries a real-valued symbol. Denoting T_0 as symbol duration and F_0 as subcarrier spacing in OFDM systems, duration and subcarrier spacing in FBMC are either $\tau_0=\frac{T_0}{2}$, $\nu_0=F_0$ or $\tau_0=T_0$, $\nu_0=\frac{F_0}{2}$ [16]. For the system model in this paper, the former approach is adopted. That is, subcarrier spacing remains the same as OFDM, while symbol duration is reduced by half.

Assuming a multiple antenna scenario with P transmit antennas, Q receive antennas, and M subcarriers, the baseband signal to be transmitted over the pth branch in general form is expressed as

$$s^{(p)}(t)=\sum_{n=-\infty}^{+\infty}\sum_{m=0}^{M-1}a_{m,n}^{(p)}g_{m,n}(t), \tag{1}$$

where $a_{m,n}^{(p)}$ is the real-valued symbol, and $g_{m,n}(t)$ is the shifted version of the prototype filter on the mth subcarrier and at nth symbol duration:

$$g_{m,n}(t)=j^{m+n}e^{j2\pi m\nu_0 t}g(t-n\tau_0). \tag{2}$$

The prototype filter $g(t)$ is designed to keep its shifted versions are orthogonal only in the real field [17], i.e.,

$$R\left(\int g_{m,n}(t)g_{m_0,n_0}^{*}(t)\mathrm{d}t\right)=\delta_{m,m_0}\delta_{n,n_0}, \tag{3}$$

where $R(.)$ denotes the real-part of a complex number. As a consequence, the outputs of the analysis filter-bank have a so-called intrinsic interference term which is pure imaginary. The demodulated signal on the qth receive antenna at a particular subcarrier and symbol point (m_0,n_0) is given by

$$y_{m_0,n_0}^{(q)}=\sum_{p=1}^{P}h_{m_0,n_0}^{q,p}a_{m_0,n_0}^{(p)}+jI_{m_0,n_0}^{(q)}+\eta_{m_0,n_0}^{(q)}, \tag{4}$$

where $h_{m_0,n_0}^{q,p}$ is channel frequency response at (m_0,n_0) between q^{th} receive and p^{th} transmit antenna, $\eta_{m_0,n_0}^{(q)}$ is the noise component at q^{th} receive antenna, and the interference term $I_{m_0,n_0}^{(q)}$ is formed as

$$jI_{m_0,n_0}^{(q)}=\sum_{p=1}^{P}\sum^{(m,n)\neq(m_0,n_0)}h_{m,n}^{q,p}a_{m,n}^{(p)}\langle g\rangle_{m,n}^{m_0,n_0}. \tag{5}$$

In (5), $\langle g\rangle_{m,n}^{m_0,n_0}$ is expressed as

$$\langle g\rangle_{m,n}^{m_0,n_0}=\int g_{m,n}(t)g_{m_0,n_0}^{*}(t)\mathrm{d}t. \tag{6}$$

Having the prototype filter $g(t)$ well localized in time and frequency, it can be assumed that the intrinsic interference is mostly due to the first-order neighbouring points. That is, (m,n) in (5) can take the values of Ω^* as follows [6]:

$$\Omega^*=\{(m_0,n_0\pm1),(m_0\pm1,n_0),(m_0\pm1,n_0\pm1)\}, \tag{7}$$

which covers the (m_0,n_0) point first-order neighbours. By assuming constant channel frequency response over (m_0,n_0) and Ω^*, we can simplify (5) as

$$jI_{m_0,n_0}^{(q)}=\sum_{p=1}^{P}h_{m_0,n_0}^{p,q}\sum^{(m,n)\in\Omega^*}a_{m,n}^{(p)}\langle g\rangle_{m,n}^{m_0,n_0}. \tag{8}$$

Consequently, (4) can be written as

$$y_{m_0,n_0}^{(q)}=\sum_{p=1}^{P}h_{m_0,n_0}^{p,q}\left(\underbrace{a_{m_0,n_0}^{(p)}+ju_{m_0,n_0}^{(p)}}_{c_{m_0,n_0}^{(p)}}\right)+\eta_{m_0,n_0}^{(p)}, \tag{9}$$

where

$$ju_{m_0,n_0}^{(p)}=\sum^{(m,n)\in\Omega^*}a_{m,n}^{(p)}\langle g\rangle_{m,n}^{m_0,n_0}. \tag{10}$$

Table 1 shows the number of $\langle g\rangle_{m,n}^{m_0,n_0}$ coefficients on the first-order neighbours of the point (m_0,n_0). The weights of interference, β, γ, and δ, depend on the prototype filter and have been derived in [18]. In this work, the isotropic orthogonal transform algorithm (IOTA) [19] filter is employed. It exploits the symmetrical property of Gaussian function in time and frequency. Therefore, the amount of interference out of first-order neighbouring points is negligible. The weights of interference for this filter are $\beta=0.2486$, $\gamma=0.5755$, and $\delta=0.1898$ (Table 1).

The MIMO-FBMC signal model can be represented as

$$\begin{pmatrix}y_{m_0,n_0}^{(1)}\\ \vdots\\ y_{m_0,n_0}^{(Q)}\end{pmatrix}=\begin{pmatrix}h_{m_0,n_0}^{1,1}&\cdots&h_{m_0,n_0}^{1,P}\\ \vdots&\ddots&\vdots\\ h_{m_0,n_0}^{Q,1}&\cdots&h_{m_0,n_0}^{Q,P}\end{pmatrix}\begin{pmatrix}c_{m_0,n_0}^{(1)}\\ \vdots\\ c_{m_0,n_0}^{(Q)}\end{pmatrix}+\begin{pmatrix}\eta_{m_0,n_0}^{(1)}\\ \vdots\\ \eta_{m_0,n_0}^{(Q)}\end{pmatrix} \tag{11}$$

where $c_{m_0,n_0}^{(p)}$ is defined in (9). To retrieve the transmitted symbols from the system above, it is necessary to have an evaluation of the channel coefficients, which are used to detect the linearly combined demodulated complex symbols $c_{m_0,n_0}^{(p)}$ at each receiver branch using zero forcing (ZF), minimum mean square error (MMSE), or maximum likelihood (ML). In $c_{m_0,n_0}^{(p)}$, the imaginary parts are intrinsic interference terms. By taking $R\{.\}$ operation, the transmitted symbols $a_{m_0,n_0}^{(p)}=R\left\{c_{m_0,n_0}^{(p)}\right\}$ are recovered.

2.2 Channel Estimation

To obtain the channel information over one frame duration on each receive antenna, we need to know the transmitted pilot symbols. The number of these pilot symbols should be equal to P to form a linear equation system with the least square estimation method. For simplicity, let us consider a 2-by-2 antenna scenario. By allocating two pilot symbols at times $n=n_0$ and $n=n_1$ on each antenna, the equation set of the system on subcarrier m is given by

$$\begin{pmatrix}y_{m,n_0}^{(1)}&y_{m,n_1}^{(1)}\\ y_{m,n_0}^{(2)}&y_{m,n_1}^{(2)}\end{pmatrix}=\begin{pmatrix}h_{m,n_0}^{1,1}&h_{m,n_0}^{1,2}\\ h_{m,n_0}^{2,1}&h_{m,n_0}^{2,2}\end{pmatrix}\begin{pmatrix}x_{m,n_0}^{(1)}&x_{m,n_1}^{(1)}\\ x_{m,n_0}^{(2)}&x_{m,n_1}^{(2)}\end{pmatrix}+\begin{pmatrix}\eta_{m,n_0}^{(1)}&\eta_{m,n_1}^{(1)}\\ \eta_{m,n_0}^{(2)}&\eta_{m,n_1}^{(2)}\end{pmatrix}. \tag{12}$$

In (12), $x_{m,n}^{(p)}$ are pilot symbols. We have assumed that there is no significant variations in the channel between time slots n_0 and n_1. Hence, we can drop the time subscript and express (12) as

$$\mathbf{Y}_m=\mathbf{H}_m\mathbf{X}_m+\boldsymbol{\eta}_m. \tag{13}$$

Thus, channel coefficients can be calculated by the least square estimation method:

$$\hat{\mathbf{H}}_m=\mathbf{Y}_m\left(\mathbf{X}_m^H\mathbf{X}_m\right)^{-1}\mathbf{X}_m^H=\mathbf{H}_m+\boldsymbol{\eta}_m\left(\mathbf{X}_m^H\mathbf{X}_m\right)^{-1}\mathbf{X}_m^H, \tag{14}$$

or in a special case with the equal number of transmit and receive antenna:

$$\hat{\mathbf{H}}_m=\mathbf{Y}_m\mathbf{X}_m^{-1}=\mathbf{H}_m+\boldsymbol{\eta}_m\mathbf{X}_m^{-1}. \tag{15}$$

The preamble in the IAM methods is composed of $2P+1$ symbols. That is, the length of the preamble grows linearly with P. The symbols with even time indices are pilots, while other symbols are all zeros to protect pilots from intrinsic interference. Based on the values of pilot symbols, i.e. real, imaginary, or complex valued pilots, IAM-R, IAM-I and IAM-C were proposed. In these approaches, the channel coefficients can be obtained using (12). For P=2, pilot symbols in (12) are set as $x_{m,n_0}^{(1)}=x_{m,n_1}^{(1)}=x_{m,n_0}^{(2)}=-x_{m,n_1}^{(2)}=x_m$. Hence, they form a system based on (12) as

$$\mathbf{Y}_m=x_m\mathbf{H}_m\begin{pmatrix}1&1\\ 1&-1\end{pmatrix}+\boldsymbol{\eta}_m=x_m\mathbf{H}_m\mathbf{A}_2+\boldsymbol{\eta}_m, \tag{16}$$

where $\mathbf{A}_2=\mathbf{A}_2^{-1}$ is an orthogonal matrix if omitting the constant coefficient of the inverse [14]. Finally, the channel coefficients are obtained as follows:

$$\hat{\mathbf{H}}_m=\frac{1}{x_m}\mathbf{Y}_m\mathbf{A}_2=\mathbf{H}_m+\frac{1}{x_m}\boldsymbol{\eta}_m\mathbf{A}_2. \tag{17}$$

The length of the preamble in this method is $2P+1=5$ with just two pilot symbols. As a result, this approach suffers from significant pilot overhead which reduces the spectral efficiency. Furthermore, the periodic nature of the pilots in these preambles results in high PAPR at the output of the synthesis filter-

▼**Table 1. Weights of interference on the first-order neighbours**

	n_0-1	n_0	n_0+1
m_0-1	$(-1)^{m_0}\delta$	$-\beta$	$(-1)^{m_0}\delta$
m_0	$-(-1)^{m_0}\gamma$	1	$(-1)^{m_0}\gamma$
m_0+1	$(-1)^{m_0}\delta$	β	$(-1)^{m_0}\delta$

bank [14].

3 Proposed Method

In order to reduce the preamble overhead and accordingly increase the spectral efficiency, a novel channel estimation approach with modest computation complexity is proposed. Since there is no need to have an estimation of the channel on each subcarrier, we can reduce the number of pilot symbols to one. In this way, each subcarrier is allocated to only one branch to transmit pilot. That is, while a branch is transmitting pilot on a subcarrier, the other branches remain silent. Therefore, the channel parameters between the receive branch and the pilot transmitting branch on that specific subcarrier can be obtained. This method enables the increase of transmit branches with a constant length of the preamble.

To elaborate the system more precisely, we assume a 2x2 MIMO system where preambles for branches 1 and 2 are shown in **Fig. 1**. It can be seen that the first and third symbols are all zero to protect the preamble from intrinsic interference from data section and previous frame. In the middle symbol for branch 1, complex pilots are placed on odd subcarriers, while the other subcarriers carry zeros. On branch 2, orthogonal pilots to branch 1 are sent, i.e., even subcarriers carry complex pilots and the rest are zero valued. On a particular subcarrier $m = m_0$, the system equations is written as follows:

$$\begin{pmatrix} y_{m_0}^{(1)} \\ y_{m_0}^{(2)} \end{pmatrix} = \begin{pmatrix} h_{m_0}^{1,1} & h_{m_0}^{1,2} \\ h_{m_0}^{2,1} & h_{m_0}^{2,2} \end{pmatrix} \begin{pmatrix} x_{m_0}^{(1)} \\ x_{m_0}^{(2)} \end{pmatrix} + \begin{pmatrix} \eta_{m_0}^{(1)} \\ \eta_{m_0}^{(2)} \end{pmatrix}. \tag{18}$$

On odd subcarriers $m_0 = 2k+1$, we have $x_{m_0}^{(1)} = X_{m_0}$, while $x_{m_0}^{(2)} = 0$. Then, the channel coefficients $h_{m_0}^{1,1}$ and $h_{m_0}^{2,1}$ are obtained as

$$\begin{aligned} h_{m_0}^{1,1} &= \frac{y_{m_0}^{(1)}}{X_{m_0}} \Big|_{x_{m_0}^{(2)}=0} \\ h_{m_0}^{2,1} &= \frac{y_{m_0}^{(2)}}{X_{m_0}} \Big|_{x_{m_0}^{(2)}=0}. \end{aligned} \tag{19}$$

Likewise, on even subcarriers the channel coefficients of $h_{m_0}^{1,2}$ and $h_{m_0}^{2,2}$ are given by

$$\begin{aligned} h_{m_0}^{1,2} &= \frac{y_{m_0}^{(1)}}{X_{m_0}} \Big|_{x_{m_0}^{(1)}=0} \\ h_{m_0}^{2,2} &= \frac{y_{m_0}^{(2)}}{X_{m_0}} \Big|_{x_{m_0}^{(1)}=0}. \end{aligned} \tag{20}$$

Hence, we have calculated the channel parameters between each pair of antennas on alternative subcarriers. Channel Coefficients on the rest of subcarriers can be obtained by interpolation. Due to short distance between pilots in this system, linear interpolation provides enough accuracy with the advantage of low complexity.

The technique works perfectly for MIMO - OFDM systems [15]. When applying this method to MIMO-FBMC, intrinsic interference degrades the channel estimation performance, i.e., transmitted pilots from one branch interfere with the received pilots on other branch. Consequently, the conditions in (19) and (20) no longer hold. To tackle this problem, we propose a precoding approach in which the interference is calculated at the transmitter side. Then, the zero points in pilot symbols are replaced by $I_{m,n}$, so that there are no interference on the corresponding points at the receiver side. That is, the pilots are received without any interference from other branches.

Fig. 2 shows the precoded pilots. The value of cancelling interference on subcarrier m is calculated by using (10) as

$$I_{m,n} = -\sum_{(m',n')\in\Omega^*} a_{m,n}^{(p)} \langle g \rangle_{m,n}^{m',n'}. \tag{21}$$

Moreover, the adjacent points of the pilot X_m are filled with pre-calculated values to maximize the received signal energy, thereby to enhance the estimation accuracy [18]. Defining $X_m = X_m^R + jX_m^I$, These values would be

$$\begin{aligned} X_m' &= -jX_m^I \\ X_m'' &= -X_m^R. \end{aligned} \tag{22}$$

Consequently, the amplitude of the real and imaginary parts

0	X_{m-3}	0	0	0	0
0	0	0	0	X_{m-2}	0
0	X_{m-1}	0	0	0	0
0	0	0	0	X_m	0
0	X_{m+1}	0	0	0	0
0	0	0	0	$X\_(m+2)$	0
	Branch 1			Branch 2	

▲**Figure 1. The basic preamble for two antennas.**

X_{m-3}'	X_{m-3}	X_{m-3}^*	0	$I_{m-3,1}$	0
0	$I_{m-2,1}$	0	X_{m-2}'	X_{m-2}	X_{m-2}''
X_{m-1}'	X_{m-1}	X_{m-1}^*	0	$I_{m-1,1}$	0
0	$I_{m,1}$	0	X_m'	X_m	X_m^*
X_{m+1}'	X_{m+1}	X_{m+1}^*	0	$I_{m+1,1}$	0
0	$I_{m+2,1}$	0	X_{m+2}'	X_{m+2}	X_{m+2}''
	Branch 1			Branch 2	

▲**Figure 2. The preambles for two antennas after interference cancellation of the first and third time symbols that helps the pilots become stronger.**

of the received pilots becomes

$$\begin{aligned}\left|\hat{X}_m^R\right| &= \left|X_m^R\right| + \gamma\left|X_m^{'}\right| + \gamma\left|X_m^I\right| \\ \left|\hat{X}_m^I\right| &= \left|X_m^I\right| + \gamma\left|X_m^{''}\right| + \gamma\left|X_m^R\right|\end{aligned}, \tag{23}$$

where γ is the interference weight shown in Table 1. The complete design of the preambles is displayed in Fig. 2. The pilots can take arbitrary values. In this work, the maximum amplitude of the used QAM modulation is used so that $X_m^R = X_m^I$. In order to avoid high PAPR, the sign of the pilots should be changed alternatively after a number of repetitions. The final value of the received pilots in (23) with $X_m^R = X_m^I$ is

$$\hat{X}_m = (1+2\gamma)X_m. \tag{24}$$

The extension to P-branch MIMO system is straightforward. In this case, one subcarrier of every P subcarriers carries a pilot (non-zero), while each branch's pilot symbol is orthogonal to other branches. The more transmit branches, the more distance between pilot subcarriers. Consequently, for larger number of branches, the quality of channel estimation degrades.

4 Simulation Results

In this section, different preamble-based channel estimators for a 2x2 MIMO-FBMC system are simulated and compared. The simulations are performed using 7-tap EPA-5Hz and 9-tap ETU-70Hz channel models with low spatial correlations. Perfect synchronization is assumed for BER and MSE comparison, i.e., there is no timing or frequency offset errors. In order to detect symbols, MMSE equalizer is used. **Table 2** summarizes the simulation parameters.

The results are compared with IAM-R and IAM-C methods introduced in [14]. For fair comparison, the transmission power is kept equal for all methods. In this system, $\frac{E_b}{N_0}$ is defined by

$$\frac{E_b}{N_0} = Q\frac{SNR}{\alpha \times \log_2(M)}, \tag{25}$$

where $M = 16$ is the modulation order, SNR is signal-to-noise ratio, and $\alpha = N_s - \frac{N_p}{N_s}$ with the frame length $N_s = 14$ and the preamble length N_p. The length of preamble N_p in the proposed method is three symbols resulting in 40% overhead reduction compared to IAMs. As a result, a performance gain is expected due to shorter preamble. The extra symbols generated by the synthesis filter-banks can be dropped before transmission, but one of them with the most power should be kept to avoid filtering errors after demodulation, i.e., $N_s + 1$ symbols are transmitted. To consider this extra symbol, α can be changed to $\alpha = N_s - \frac{N_p}{N_s} + 1$.

▼**Table 2. Simulation parameters**

Modulation type	M-QAM, M =16
FFT size	256
Used subcarriers	144
Sampling frequency	3.84 MHz
Symbols per frame	14
Channel	EPA 5 Hz, ETU 70 Hz

EPA: Extended Pedestrian A model
ETU: Extended Typical Urban model
FFT: fast Fourier transform
QAM: quadrature amplitude modulation

4.1 PAPR Comparison

Fig. 3 shows the comparison between the proposed method and IAMs in terms of PAPR. The plots show the squared magnitude of the preambles at the output of the synthesis filter-bank on branch 1. Evidently, from the point of practical implementations, the proposed method is preferable. Whereas in the others, the signal level should be kept very low to avoid A/D saturations. The PAPR levels for the pilot symbols are compared in **Table 3** for the three methods.

4.2 Channel Estimation Performance Comparison

Fig. 4 shows the MSE comparison of the channel estimation methods. To calculate MSE, the channel tap on the second symbol in frame is considered as reference and it is assumed constant during the symbol duration. Then, the MSE is calcu-

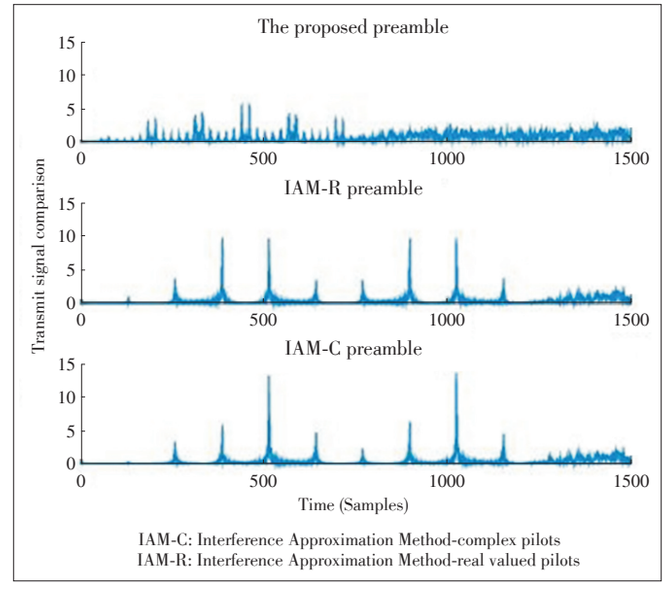

IAM-C: Interference Approximation Method-complex pilots
IAM-R: Interference Approximation Method-real valued pilots

▲**Figure 3. Squared magnitude of the preambles on output of the branch 1.**

▼**Table 3. PAPR comparison for the three methods**

	IAM-C	IAM-R	Proposed
PAPR	17.5	9.3	7.2

IAM-C: Interference Approximation Method-complex pilots
IAM-R: Interference Approximation Method-real valued pilots
PAPR: peak to average power ratio

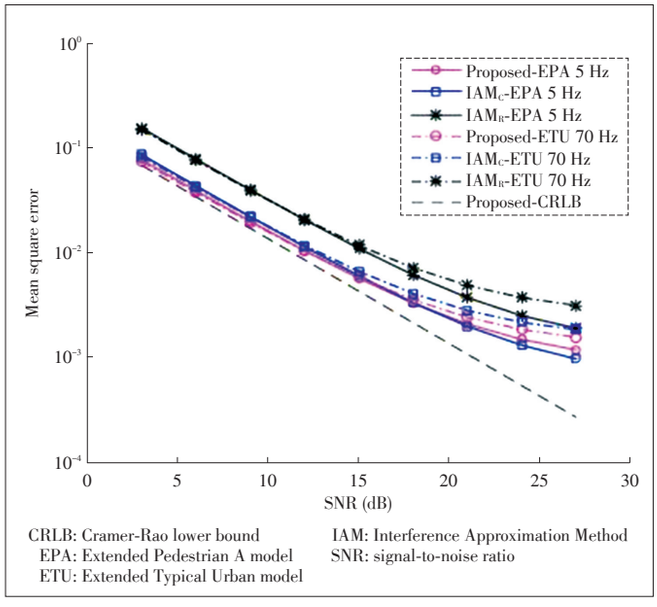

▲Figure 4. MSE performance of the channel estimation methods.

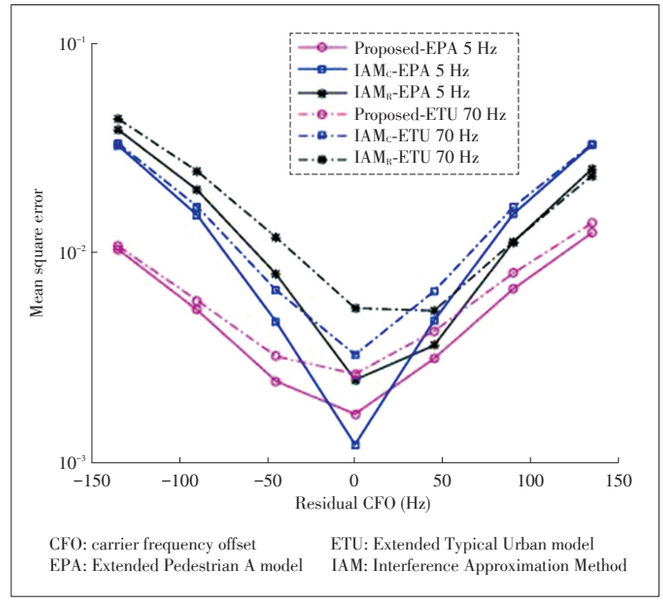

▲Figure 5. MSE performance of the channel estimation methods in presence of residual CFO.

lated using the estimated channel $\hat{\mathbf{H}}$ as $\mathbf{E}\left(\left(\mathbf{H}-\hat{\mathbf{H}}\right)^{H}\left(\mathbf{H}-\hat{\mathbf{H}}\right)\right)$. It can be seen that the proposed preamble outperforms IAM-R and has approximately the same performance as IAM-C in both channel models. In the EPA-5Hz scenario, the proposed method gradually reaches an error floor. This is due to domination of errors from ISI and interference cancellation residual. However, the performance is still as good as IAM-C. In the ETU-70Hz scenario, because of rapid variation of the channel taps, the assumption of constant channel over Ω^{*} in (8) is invalid. Consequently, the performance of all the methods degrades and reaches an error floor in higher SNRs. This is a general problem in channel estimation for FBMC systems where the receiver should necessarily have an estimation of intrinsic interferences for channel estimation. However, the degradation on IAMs is more significant as the channel is estimated using two symbols with one zero symbol in between. Therefore, as the channel is not constant over the two pilot symbols, degradation is higher than the proposed method with only one symbol for channel estimation. The Cramer-Rao lower bound (CRLB) for the proposed method, derived in Appendix A has also been plotted in the figure for benchmark comparison. It can be seen that the proposed scheme achieves closest performance to the theoretical lower bound in comparison to the other schemes.

Fig. 5 shows the MSE comparisons in terms of residual CFO. It is assumed that the CFO has been estimated and compensated before channel estimation. As the estimated CFO is not perfect, the residual CFO affects the quality of channel estimation. Therefore, the methods are compared in presence of residual CFO in the two channel scenarios without added white Gaussian noise. When the CFO is zero, the MSEs show the error floor of the methods in Fig. 4 at very high SNRs. It can be seen that in EPA channel, the error floor of the proposed method is higher than IAM-C, while it has the best performance under ETU channel. This is also true for the other values of CFO, where the degradation of MSE in the proposed method is lower than the other two in both channels.

4.3 Bit Error Rate Performance Comparison

The BER performance comparison with respect to $\frac{E_b}{N_0}$ is illustrated in **Fig. 6**. Evidently, the proposed method performs

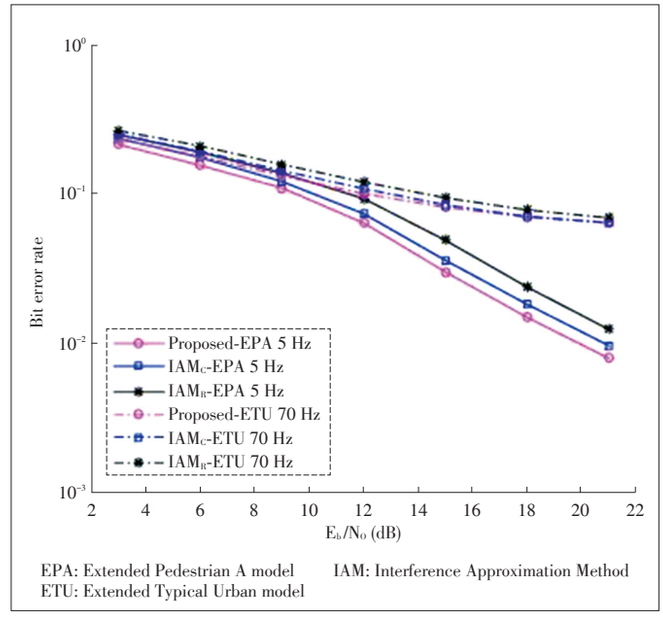

▲Figure 6. BER performance of the channel estimation methods.

better compared to the others in low mobility EPA-5Hz scenario. In the high mobility ETU-70Hz channel, the performance deteriorates as the channel varies significantly during the frame time. Consequently, the preamble-based channel estimation is not a proper choice for high mobility applications and there is an error floor for all the curves showing around six percent bit error rate.

5 Conclusions

In this paper, we proposed a novel channel estimation algorithm with much reduced pilot overhead compared to the existing IAM based approaches. Our results show that the proposed method has better PAPR property. The system performance under low mobility and high mobility channels, as well as in the presence of CFO, has been simulated and compared. According to the results, the proposed method achieves comparable channel estimation performance to the IAM methods, and better BER performance due to shorter preamble.

Appendix A

Cramer-Rao Lower Bound for the Proposed Channel Estimation

In this section, a lower bound for the proposed channel estimator is derived. We simplify the system using equations (13), (18), (19), and (20) as

$$\mathbf{Y} = X\mathbf{H} + \boldsymbol{\eta}, \tag{26}$$

where $\mathbf{Y} = [y_1\ y_2]$ is the received signal vector, $\boldsymbol{\eta} = [\eta_1\ \eta_2]$ is the noise vector, $\mathbf{H} = [h_1\ h_2]$ is the channel vector to be estimated, X is the pilot symbol. The subcarrier index has also been dropped for simplicity.

The CRLB is a bound on the smallest covariance matrix that can be achieved by an unbiased estimator, $\hat{\mathbf{H}}$, of a parameter vector $\mathbf{H}$ as

$$\begin{aligned}&\mathbf{J}^{-1} \leqslant \mathbf{C}_{\hat{\mathbf{H}}} = \mathrm{E}\left\{\left(\mathbf{H}-\hat{\mathbf{H}}\right)\left(\mathbf{H}-\hat{\mathbf{H}}\right)^{*}\right\};\\ &\mathbf{J} = \mathrm{E}\left\{\left(\frac{\partial \ln p(\mathbf{Y};\mathbf{H})}{\partial \mathbf{H}}\right)\left(\frac{\partial \ln p(\mathbf{Y};\mathbf{H})}{\partial \mathbf{H}}\right)^{*}\right\},\end{aligned} \tag{27}$$

where $(\cdot)^{*}$ denotes conjuagate transpose operation, $\mathbf{J}$ is the Fisher information matrix and $\ln p(\mathbf{Y};\mathbf{H})$ is the log-likelihood function of the observed vector $\mathbf{Y}$. The vector $\mathbf{Y}$ is a complex Gaussian random vector, i.e., $\mathbf{Y} \sim CN(X\mathbf{H}, N_0\mathbf{I})$ with likelihood function and log-likelihood function as

$$\begin{aligned}&(\mathbf{Y};\mathbf{H}) = \frac{1}{(\pi N_0)^2}\exp\left[-\frac{(\mathbf{Y}-X\mathbf{H})^{*}(\mathbf{Y}-X\mathbf{H})}{N_0}\right] =\\ &\frac{1}{(\pi N_0)^2}\exp\left[-\frac{\|\mathbf{Y}\|^2 - \mathbf{H}^{*}X^{*}\mathbf{Y} - \mathbf{Y}^{*}X\mathbf{H} + \mathbf{H}^{*}X^{*}X\mathbf{H}}{N_0}\right];\\ &\ln p(\mathbf{Y};\mathbf{H}) = K - \frac{\|\mathbf{Y}\|^2 - \mathbf{H}^{*}X^{*}\mathbf{Y} - \mathbf{Y}^{*}X\mathbf{H} + \mathbf{H}^{*}X^{*}X\mathbf{H}}{N_0},\end{aligned} \tag{28}$$

where K is a constant. Taking the complex gradient [20] of $\ln p(\mathbf{Y};\mathbf{H})$ with respect to $\mathbf{H}$ yields

$$\frac{\partial \ln p(\mathbf{Y};\mathbf{H})}{\partial \mathbf{H}} = -\frac{1}{N_0}\left[X^{*}X\mathbf{H} - X^{*}\mathbf{Y}\right]^{*}. \tag{29}$$

The above equality holds since

$$\begin{aligned}&\frac{\partial \|\mathbf{Y}\|^2}{\partial \mathbf{H}} = 0; \qquad \frac{\partial \mathbf{H}^{*}X^{*}\mathbf{Y}}{\partial \mathbf{H}} = 0;\\ &\frac{\partial \mathbf{Y}^{*}X\mathbf{H}}{\partial \mathbf{H}} = \left(X^{*}\mathbf{Y}\right)^{*}; \frac{\partial \mathbf{H}^{*}X^{*}X\mathbf{H}}{\partial \mathbf{H}} = \left(X^{*}X\mathbf{H}\right)^{*}.\end{aligned} \tag{30}$$

Thus we can derive,

$$\begin{aligned}&\frac{\partial \ln p(\mathbf{Y};\mathbf{H})}{\partial \mathbf{H}^{*}} = \left(\frac{\partial \ln p(\mathbf{Y};\mathbf{H})}{\partial \mathbf{H}}\right)^{*} = \frac{X^{*}\mathbf{Y} - X^{*}X\mathbf{H}}{N_0} =\\ &\frac{X^{*}X}{N_0}\left\{\left(X^{*}X\right)^{-1}X^{*}\mathbf{Y} - \mathbf{H}\right\} = \mathbf{J}(\mathbf{H})\left[\hat{\mathbf{H}} - \mathbf{H}\right].\end{aligned} \tag{31}$$

This proves that the minimum variance unbiased estimator of $\mathbf{H}$ is

$$\hat{\mathbf{H}} = \left(X^{*}X\right)^{-1}X^{*}\mathbf{Y} = \frac{\mathbf{Y}}{X}. \tag{32}$$

It is efficient in that it attains the CRLB. The Fisher information matrix $\mathbf{J}(\mathbf{H})$ and covariance matrix $\mathbf{C}_{\hat{\mathbf{H}}}$ of this unbiased estimator are

$$\begin{aligned}&\mathbf{J}(\mathbf{H}) = \mathrm{E}\left[\frac{X^{*}X\mathbf{I}_2}{N_0}\right] = \frac{\mathrm{E}\left[X^{*}X\right]\mathbf{I}_2}{N_0} = \frac{E_x}{N_0}\mathbf{I}_2\\ &\mathbf{C}_{\hat{\mathbf{H}}} = \mathbf{J}^{-1}(\mathbf{H}) = \frac{N_0}{\mathrm{E}_x}\mathbf{I}_2.\end{aligned} \tag{33}$$

In (33), E_x is the pilot energy. The CRLB for each diagonal element of $\mathbf{J}^{-1}(\mathbf{H})$ is

$$\mathrm{var}\left(\hat{h}_1\right) = \mathrm{var}\left(\hat{h}_2\right) = \mathrm{diag}\left[\mathbf{C}_{\hat{\mathbf{H}}}\right]_i = \frac{N_0}{E_x}. \tag{34}$$

As the pilots in this system are amplified exploiting intrinsic interference by the factor of $1+2\gamma$, E_x should be replaced by $E_x^{'} = (1+2\gamma)^2 E_x$. Assuming $\frac{E_x}{N_0}$ is approximately equal to SNR and considering (25), (34) becomes

$$\mathrm{var}\left(\hat{h}_1\right) = \mathrm{var}\left(\hat{h}_2\right) = \frac{N_0}{E_x}\frac{1}{(1+2\gamma)^2}. \tag{35}$$

References

[1] A. Sahin, I. Guvenc, and H. Arslan, "A survey on multicarrier communications: Prototype filters, lattice structures, and implementation aspects," *IEEE Communications Surveys Tutorials*, vol. 16, no. 3, pp. 1312–1338, Mar. 2014.

[2] B. Farhang-Boroujeny, "OFDM versus filter bank multicarrier," *IEEE Signal Processing Magazine*, vol. 28, no. 3, pp. 92–112, May 2011.
[3] F. Schaich and T. Wild, "Waveform contenders for 5G—OFDM vs. FBMC vs. UFMC," in *6th International Symposium on Communications, Control and Signal Processing*, Athens, Greece, 2014, pp. 457 – 460. doi: 10.1109/ISCCSP.2014.6877912.
[4] Q. Bai and J. Nossek, "On the effects of carrier frequency offset on cyclic prefix based OFDM and filter bank based multicarrier systems," in *IEEE Eleventh International Workshop on Signal Processing Advances in Wireless Communications*, Marrakech, Morocco, Jun. 2010, pp. 1–5. doi: 10.1109/SPAWC.2010.5670999.
[5] M. Sriyananda and N. Rajatheva, "Analysis of self interference in a basic FBMC system," in *IEEE 78th Vehicular Technology Conference*, Las Vegas, USA, Sept. 2013, pp. 1–5. doi: 10.1109/VTCFall.2013.6692102.
[6] J. Javaudin and Y. Jiang, "Channel estimation in MIMO OFDM/OQAM," in *IEEE 9th Workshop on Signal Processing Advances in Wireless Communications*, Recife, Brazil, Jul. 2008, pp. 266–270. doi: 10.1109/SPAWC.2008.4641611.
[7] J. Javaudin, D. Lacroix, and A. Rouxel, "Pilot-aided channel estimation for OFDM/OQAM," in *57th IEEE Semiannual Vehicular Technology Conference*, Jeju, South Korea, Apr. 2003, pp. 1581–1585. doi: 10.1109/VETECS.2003.1207088.
[8] C. Lele, R. Legouable, and P. Siohan, "Channel estimation with scattered pilots in OFDM/OQAM," in *IEEE 9th Workshop on Signal Processing Advances in Wireless Communications*, Recife, Brazil, Jul. 2008, pp. 286–290. doi: 10.1109/SPAWC.2008.4641615.
[9] Z. Zhao, N. Vucic, and M. Schellmann, "A simplified scattered pilot for FBMC/OQAM in highly frequency selective channels," in *11th international symposium on Wireless communications systems*, Barcelona, Spain, Oct. 2014, pp. 819–823. doi: 10.1109/ISWCS.2014.6933466.
[10] J. Bazzi, P. Weitkemper, and K. Kusume, "Power efficient scattered pilot channel estimation for FBMC/OQAM," in *10th International ITG Conference on Systems, Communications and Coding*, Hamburg, Germany, Feb. 2015, pp. 1–6.
[11] C. Lélé, J. Javaudin, R. Legouable, A. Skrzypczak, and P. Siohan, "Channel estimation methods for preamble-based OFDM/OQAM modulations," *Transactions on Emerging Telecommunications Technologies*, pp. 741–750, Sept. 2008. doi: 10.1002/ett.1332.
[12] C. Lélé, P. Siohan, and R. Legouable, "2 dB better than CP-OFDM with OFDM/OQAM for preamble-based channel estimation," in *IEEE International Conference on Communications*, Beijing, China, 2008, pp. 1302–1306. doi: 10.1109/ICC.2008.253.
[13] J. Du and S. Signell, "Novel preamble-based channel estimation for OFDM/OQAM systems," in *IEEE International Conference on Communications*, Dresden, Germany, 2009, pp. 1–6. doi: 10.1109/ICC.2009.5199226.
[14] E. Kofidis and D. Katselis, "Preamble-based channel estimation in MIMO-OFDM/OQAM systems," in *IEEE International Conference on Signal and Image Processing Applications*, Kuala Lumpur, Malaysia, 2011, pp. 579–584. doi: 10.1109/ICSIPA.2011.6144161.
[15] J. Siew, R. Piechocki, A. Nix, and S. Armour. (2002). "A channel estimation method for MIMO-OFDM systems," *London Communicaitons Symposium (LCS)* [Online]. Available: http://www.ee.ucl.ac.uk/lcs/previous/LCS2002/LCS087.pdf
[16] J. Du, P. Xiao, J. Wu, and Q. Chen, "Design of isotropic orthogonal transform algorithm-based multicarrier systems with blind channel estimation," *IET communications*, vol. 6, no. 16, pp. 2695–2704, Nov. 2012. doi: 10.1049/iet-com.2012.0029.
[17] P. Siohan, C. Siclet, and N. Lacaille, "Analysis and design of OFDM/OQAM systems based on filterbank theory," *IEEE Transactions on Signal Processing*, vol. 50, no. 5, pp. 1170–1183, May 2002.
[18] E. Kofidis and D. Katselis, "Improved interference approximation method for preamble-based channel estimation in FBMC/OQAM," in *19th European signal processing conference (EUSIPCO-2011)*, Barcelona, Spain, 2011. pp. 1603–1607.
[19] J. Du and S. Signell, "Time frequency localization of pulse shaping filters in OFD/OQAM systems," in *6th International Conference on Information, Communications Signal Processing*, Singapore, 2007, pp. 1–5.
[20] S. Kay, *Fundamentals of Statistical Signal Processing*. Upper Saddle River, USA: Prentice Hall, 1998.

Manuscript received: 2016-04-04

Biographies

Sohail Taheri (s.taheri@surrey.ac.uk) received his BS degree in electronic engineering and MSc degree in digital electronics from Amirkabir University of Technology, Iran in 2010 and 2012 respectively. He is currently working towards his PhD degree from the Institute for Communication Systems (ICS), University of Surrey, United Kingdom. His current research interests include signal processing for wireless communications, waveform design for 5G air interface and physical layer for 5G networks.

Mir Ghoraishi (m.ghoraishi@surrey.ac.uk) is a senior research fellow in the Institute for Communication Systems (ICS), University of Surrey. He joined the Institute in 2012 and is currently leading 5GIC testbed and proof-of-concept projects. This work area includes several implementation and proof-of-concept projects, e.g. 5G air-interface proof-of-concept, distributed massive MIMO implementation, wireless in-band full-duplex, millimeter wave hybrid beamforming system, and millimeter wave wireless channel analysis and modelling. He was involved in EU FP7 DUPLO project as work package leader. He has previously worked in Tokyo Institute of Technology as assistant professor and senior researcher from 2004 to 2012, after getting his PhD from the same institute. In Tokyo Tech he was involved in several national and small scale projects in planning, performing, implementation, analysis and modelling different aspect of wireless systems in physical layer, propagation channel and signal processing. He has co-authored 100 publications including refereed journals, conference proceedings and three book chapters.

XIAO Pei (p.xiao@surrey.ac.uk) received the BEng, MSc and PhD degrees from Huazhong University of Science & Technology, Tampere University of Technology, Chalmers University of Technology, respectively. Prior to joining the University of Surrey in 2011, he worked as a research fellow at Queen's University Belfast and had held positions at Nokia Networks in Finland. He is a Reader at University of Surrey and also the technical manager of 5G Innovation Centre (5GIC), leading and coordinating research activities in all the work areas in 5GIC. Dr Xiao's research interests and expertise span a wide range of areas in communications theory and signal processing for wireless communications. He has published 160 papers in refereed journals and international conferences, and has been awarded research funding from various sources including Royal Society, Royal Academy of Engineering, EU FP7, Engineering and Physical Sciences Research Council as well as industry.

CAO Aijun (cao.aijun@zte.com.cn) is a principal architect in ZTE R&D Center, Sweden (ZTE Wistron Telecom AB). He has over 17 years of experience in wireless communications research and development from baseband processing to network architecture, including design and optimization of commercial UMTS/LTE base-station and handset products, HetNet and small cell enhancement, etc. He has also been involved in standardization works and contributed to several 3GPP technical reports. He is also active in academic and industrial workshops and conferences related to the future wireless networks being as panelists or (co-)authors of published papers in refereed journals and international conferences. In addition, he holds more than 50 granted or pending patents. His current focus is 5G technologies related to the new energy-efficient unified air-interface and network architecture, e.g., new waveform design, non-orthogonal multiple access schemes, random access challenges and innovative signaling architecture for 5G networks.

GAO Yonghong (gao.yonghong@zte.com.cn) received his BEng degree in electronic engineering from Tsinghua University, China in 1989, and PhD degree in electronic systems from Royal Institute of Technology, Sweden in 2001. In 1996, he was a visiting scientist at Royal Institute of Technology and Ericsson Sweden. In 1999, he joined Ericsson Sweden to develop 3G base stations, baseband algorithms, and baseband ASICs. He joined ZTE European Research Institute (ZTE Wistron Telecom AB, Sweden) in 2002 and has been the CTO of ZTE European Research Institute till now, leading and participating the development of 3G/4G commercial base stations, baseband/RRM algorithms, and baseband ASICs, 3GPP small cell enhancement, and from 3 years ago focusing on 5G pre-study, 5G standardization, and 5G research projects in Europe. He has filed 40+ patents as a main author or co-author. His research interests include mobile communication standards/systems, and solutions and algorithms for commercial wireless products.